

# XCOM and EpiXS evaluation of cosmic radiation shielding effectiveness of cerium oxide and bismuth oxide doped nanocoating for satellite applications

Toni Beth Guatato-Lopez,<sup>\*1,3</sup> Alvie Asuncion-Astronomo,<sup>2</sup> Gil Nonato C. Santos,<sup>3</sup>  
Christopher T. Que,<sup>3</sup> Dominic P. Guaña,<sup>1</sup> and Paul Leonard Atchong Hilario<sup>1</sup>

<sup>1</sup>Philippine Space Agency, 29F CyberOne Building, 11 Eastwood Ave., Bagumbayan, Quezon City

<sup>2</sup>DOST–Philippine Nuclear Research Institute, Commonwealth Ave., Diliman, Quezon City

<sup>3</sup>Physics Department, De La Salle University, 2401 Taft Ave., Malate, Manila

\*Corresponding author: [toni.lopez@philsa.gov.ph](mailto:toni.lopez@philsa.gov.ph)

## Abstract

We investigated a potential coating material that incorporates cerium and bismuth oxides in a polymer matrix. Radiation shielding parameters, such as mass attenuation coefficient ( $\mu/\rho$ ), mean free path (mfp), and half-value layer (HVL), of this composite material with respect to various concentrations of cerium oxide and bismuth oxide in the vinyl ester matrix were calculated using XCOM and EpiXS. Results indicate that, compared to a bare polymer, the mass attenuation coefficient, measured at 1 GeV photon energy, increased by 109% when the composite has a cerium oxide concentration of 40% w/v. This confirms the performance of cerium oxide as good radiation shielding filler for higher energy ranges such as cosmic radiation.

Keywords: cosmic radiation shielding, solar cosmic rays, lens browning effect, XCOM, EpiXS

## 1 Introduction

Satellites serve various purposes such as tracking, location determination [1], atmospheric observation [2], and data transmission [3]. Positioned kilometers above Earth's surface, satellites in low Earth orbit (LEO) face risks due to the thin atmosphere. Micro and small satellites are particularly vulnerable to cosmic radiation and its damaging effects on electronics and lenses [1], [4]. Coating the satellite covering provides a flexible solution, shielding it from unnecessary cosmic radiation while allowing useful electromagnetic waves for data transfer [5]. Using metal and ceramic coatings on a polymer matrix shows potential in addressing these concerns. Rather than using heavy metals, coatings are lightweight, have minimal impact on mass loading, prolong surface life, and protect against abrasions.

Nanomaterials such as cerium oxide [6] and bismuth oxide [5] have shown promising results as fillers for radiation shielding coatings. By incorporating these nanoparticles into coatings, radiation attenuation is improved due to their high atomic number and interaction with photons. This provides effective protection against harmful radiation effects, including browning effects on satellite lenses. Browning effect on lenses is the discoloration of the lenses when continuously exposed to radiation [7].

In this paper, the use of cerium-doped bismuth oxide nanoparticles as fillers in coatings for radiation shielding was investigated using XCOM software from the National Institute of Standards and Technology (NIST) [8], USA, and EpiXS software developed by the Philippine Nuclear Research Institute (PNRI) [9].

## 2 Methodology

Cerium and bismuth oxides concentrations incorporated into the nanocomposite were varied to determine the most effective combination for shielding applications. The mass loading ratio of the composite is uniform for all concentrations which is 50% (m/v) total metal oxide to the polymer matrix, as presented in Table 1. Simulation of the mass attenuation coefficient ( $\mu/\rho$ ) was carried out using XCOM and EpiXS. The features of XCOM and EpiXS were presented in Table 2. The mean free path (mfp) and half value layer (HVL) were post-processed using Microsoft Excel from the calculation of XCOM and EpiXS. Both XCOM and EpiXS parameters were plotted to the energy range of 100 to 1000 MeV, corresponding to the energy range of cosmic radiation in space.

Both EpiXS and XCOM simulate Photoelectric absorption, Compton scattering, and Pair production because they both model high energy radiation that are characterized by inelastic scattering. Since Rayleigh scattering is a type of elastic scattering which occurs in photon-electron interaction and it is conversely related to the focus of the

calculation, therefore, it is not considered in the calculations of EpiXS. Both are derived from the Monte Carlo N-particle codes. The parameters of the calculations were based on extensive empirical data, including the geometry, density of the material, thickness, and other possible variable in calculating the interaction, and theoretical calculations incorporating to theoretical model to simulate the probable photon interaction. In this regard, the calculations are considered the best estimate of the background effects of photon interactions with the nucleus or nucleons.

Table 1: Sample ID and its corresponding mass-volume concentration and theoretical density

Sample ID	Vinyl Ester	CeO <sub>2</sub>	Bi <sub>2</sub> O <sub>3</sub>	Density (g/cc)
Vinyl Ester	100%	0%	0%	1.80
S1	50%	10%	40%	2.97
S2	50%	20%	30%	2.95
S3	50%	25%	25%	2.94
S4	50%	30%	20%	2.93
S5	50%	40%	10%	2.90

Table 2: Summary of the radiation shielding effectiveness software utilized in this study

	XCOM	EpiXS
Developer	NIST	PNRI
Photoatomic Data Library	NIST Standard Reference Database 8 (XGAM)	Electron Photon Interaction Cross Sections (EPICS2017)
Functionalities	Applicable for element, compound, and mixture	Applicable for element, compound, and mixture
Photon interaction models	Photoelectric absorption, Rayleigh scattering, Compton scattering, and Pair production	Photoelectric absorption, Compton scattering, and Pair production
Reference	(Berger, et al. 2010) [8]	(Hila, et al. 2021) [9]

### 3 Results and Discussion

The theoretical density of the composite was calculated using the general equation below [8], which can be verified using ASTM D792 or ISO 1183 testing methods:

$$\rho_{com} = \frac{m_1}{V} + \frac{m_2}{V} + \dots + \frac{m_n}{V} \quad (1)$$

In equation (1),  $\rho_{com}$  refers to the composite density,  $V$  is the total volume of the composite,  $m_n$  is the mass of each material in the composite, which for this study, includes the masses of the polymer, cerium oxide, and bismuth oxide. The calculated densities for the vinyl ester and the 5 composite samples evaluated in this study are presented in Table 2. The mass attenuation coefficient calculated by the two programs are summarized in Table 3, which indicates excellent agreement between the two sets of data. However, from the data set acquired from EpiXS, have few in-between energy ranges that were not included. The XCOM has a wider energy range compared to EpiXS. The difference in the coverage of the energy ranges is with due respect to the utilized photoatomic libraries (*c.f.* Table 1)

Figure 1 presents the plot of  $(\mu/\rho)$  as a function of photon energy for all samples evaluated in this study. As expected, the  $(\mu/\rho)$  shielding performance of vinyl ester polymer is consistently lower than that of the 5 samples as the energy was increased. The  $(\mu/\rho)$  of bare to increasing mass loading of bismuth oxide have a decreasing trend with increasing photon energy from 1 keV to 10 keV. However, the trend reverses for energies higher than 100 MeV. The trend is particularly notable for S1 as it has the lowest  $(\mu/\rho)$  value among all composites for the range 1 keV to 2 keV but the trend reverses at higher energies. From 3 keV, the  $(\mu/\rho)$  of the 6 samples have consistent orders of magnitude. From Fig.1.B, there is an increasing trend of  $(\mu/\rho)$  from 0.1 to 1 GeV. In this regard, the design of the composite conveys the energy-selective radiation shielding framework [9].

Other shielding parameters that can be determined from  $(\mu/\rho)$  are the mean free path ( $mfp$ ) and half value layer ( $HVL$ ) of each sample:

$$mfp = 1/\mu \quad (2)$$

$$HVL = \ln 2 / \mu \quad (3)$$

The  $mfp$  is the average distance that a photon traverses prior to collision with another particle, while the  $HVL$  is the shielding material thickness that can reduce the intensity of photons by half. From Fig.2.A, there is a significant difference from the values of bare polymer to the  $mfp$  of nanocomposite samples for an average of 135%. The average cross-section of vinyl ester is 33.6 cm, meanwhile, for S1, S2, S3, S4, and S5, are 5.98, 6.31, 6.49, 6.68, and 7.09 cm, respectively. Meanwhile, for the HVL of the samples, a drop of 135% relative to the HVL of vinyl ester polymer compared to the HVL of the 5 different samples. This only shows that the incorporation of metal oxides plays an important role in diminishing the effective cross-sectional area of the material that can shield radiation.

Table 3: Comparison of mass attenuation coefficient acquired using EpiXS and XCOM through percent difference

	Vinyl Ester	S1	S2	S3	S4	S5
Average	0.149	0.156	0.143	0.136	0.136	0.134
Minimum %Diff	-0.189	-0.114	-0.138	-0.177	-0.195	-0.241
Maximum %Diff	0.316	1.44	0.872	1.20	1.60	2.71

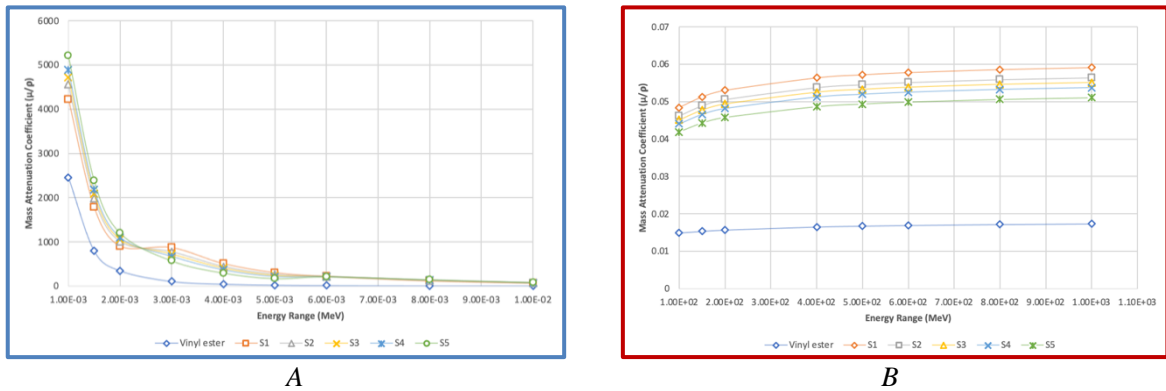


Figure 1: Mass attenuation coefficient vs. energy range graph of different concentrations of CeO<sub>2</sub> and Bi<sub>2</sub>O<sub>3</sub> incorporated in vinyl ester polymer matrix where offset graphs are from (A) 0.001-0.01 MeV energy range and (B) 100-1000 MeV.

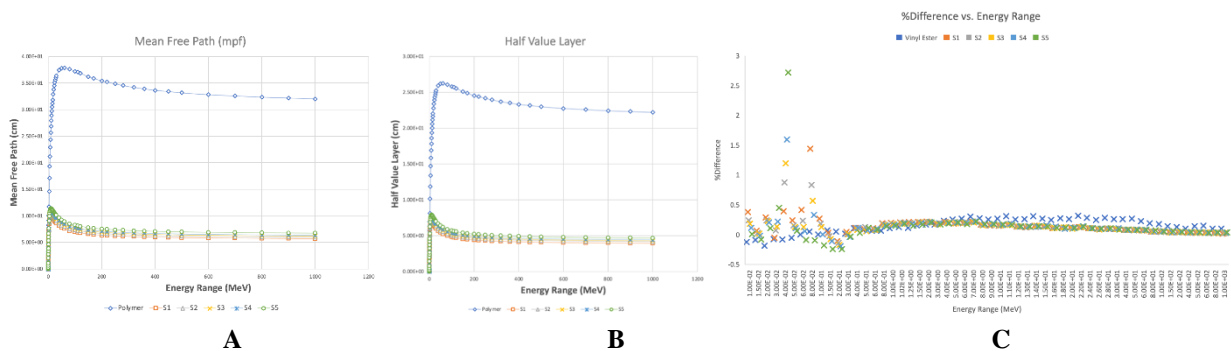


Figure 2: Graph plot for the (A) mean free path, (B) half value layer, and (C) relative percent difference of XCOM and EpiXS

## 4 Conclusions

Nanocomposites of cerium oxide and bismuth oxide in a polymer matrix were evaluated in terms of their radiation shielding effectiveness. Mass attenuation coefficient, mean free path, and half value layer are the radiation shielding parameters that were calculated using the XCOM and EpiXS programs. The percent difference as shown in Table 3 between the two data sets ranges from -0.195% to 2.71% which are considered nearly identical to each other. Using the data from EpiXS program with EPICS2017 database, the sample ID with the highest attenuation coefficient for the energy

range 0.001 to 0.01 MeV is S5, however, increasing the photon energy to 0.003 MeV, the highest attenuator changes to S1. This indicates that the ratio of bismuth oxide and cerium oxide is an energy-selective radiation shield. Since the photoelectric effect is dominant at lower photon energies, bismuth oxide exhibited better performance compared to cerium oxide because of its higher atomic number and mass density. On the other hand, cerium oxide increases the attenuation performance of the nanocomposite to higher photon energies, because pair production became significant. Since cerium has a higher atomic number, it gives a greater probability to form electron-positron which leads to energy absorption and attenuation. As for the cross-section of the nanocomposite, the incorporation of metal oxide significantly reduces the thickness of the nanocomposite which can attenuate the half value of the photon intensity. With this, the incorporation of cerium and bismuth oxide nanoparticles in a vinyl ester polymer matrix can be used for an energy-selective radiation shielding application that is suitable for space materials such as satellites.

## Acknowledgements

The authors would like to extend their gratitude to DOST PCIEERD, DOST PNRI, DLSU, and PhilSA for their unwavering support.

## References

- [1] J. Wang, Z. Huo, and F. Wang, TID evaluation based on variabilities of space radiation and device failure dose in typical navigation satellite orbits, *Microelectron. Reliab.* **137**, 114747 (2022). URL: <https://doi.org/10.1016/j.microrel.2022.114747>
- [2] E. Castro, T. Ishida, Y. Takahashi, H. Kubota, G. J. Perez, and J. S. Marciano, Determination of cloud-top height through three-dimensional cloud reconstruction using DIWATA-1 data, *Sci. Rep.* **10**, 7570 (2020). URL: <https://doi.org/10.1038/s41598-020-64274-z>
- [3] O. Kodheli, et al., Satellite communications in the new space era: A survey and future challenges, *IEEE Commun. Surv. Tutor.* **23**, 70 (2021). URL: <https://doi.org/10.1109/COMST.2020.3028247>
- [4] K. Zhang, X. Zhong, Z. Qu, Y. Meng, and Z. Su, Design method research of a radiation-resistant zoom lens, *Opt. Commun.* **509**, 127881 (2022). URL: <https://doi.org/10.1016/j.optcom.2021.127881>
- [5] B. M. Chandrika, et al., Synthesis, physical, optical and radiation shielding properties of Barium-Bismuth Oxide Borate—A novel nanomaterial, *Nucl. Eng. Technol.* **55**, 1783 (2023). URL: <https://doi.org/10.1016/j.net.2023.01.012>
- [6] E. Ilik, G. Kilic, U. G. Issever, S. A. M. Issa, H. M. H. Zakaly, and H. O. Tekin, Cerium (IV) oxide reinforced Lithium-Borotellurite glasses: A characterization study through physical, optical, structural and radiation shielding properties, *Ceram. Int.* **48**, 1152 (2022). URL: <https://doi.org/10.1016/j.ceramint.2021.09.200>
- [7] Radiation Induced Discoloration, (Birns, Inc., 2023), <http://birns.com/uploads/file/Radiation-induced%20Discoloration.pdf>, accessed 21 Jun 2023 .
- [8] M. J. Berger, et al., XCOM: Photon Cross Sections Database, *NIST Standard Reference Database 8 (XGAM)*, (NIST, 2010). URL: <https://doi.org/10.18434/T48G6X>
- [9] F. C. Hila, et al., EpiXS: A Windows-based program for photon attenuation, dosimetry and shielding based on EPICS2017 (ENDF/B-VIII) and EPDL97 (ENDF/B-VI.8), *Radiat. Phys. Chem.* **182**, 109331 (2021). URL: <https://doi.org/10.1016/j.radphyschem.2020.109331>